Article

Optical Detection of Enzymatic Activity and Inhibitors on Non-Covalently Functionalized Fluorescent Graphene Oxide

Tae Woog Kang, Su-Ji Jeon, Hye-In Kim, Jung Hyun Park, DaBin Yim, Hye-Rim Lee, Jong-Min Ju, Man-Jin Kim, and Jong-Ho Kim

ACS Nano, **Just Accepted Manuscript** • DOI: 10.1021/acsnano.6b01495 • Publication Date (Web): 02 May 2016

Optical Detection of Enzymatic Activity and Inhibitors on Non-Covalently Functionalized Fluorescent Graphene Oxide

*Tae Woog Kang, Su-Ji Jeon, Hye-In Kim, Jung Hyun Park, DaBin Yim, Hye-Rim Lee, Jong-Min Ju, Man-Jin Kim and Jong-Ho Kim**

Department of Chemical Engineering, Hanyang University, Ansan 426-791, Republic of Korea

*To whom correspondence should be addressed: kjh75@hanyang.ac.kr

ABSTRACT

It has been of great interest to measure the activity of acetylcholinesterase (AChE) and its inhibitor, as AChE is known to accelerate the aggregation of the amyloid beta peptides that underlie Alzheimer's disease. Herein, we report the development of graphene oxide (GO) fluorescence-based biosensors for the detection of AChE activity and AChE inhibitors. To this end, GO was non-covalently functionalized with phenoxy-modified dextran (PhO-dex-GO) through hydrophobic interaction; the resulting GO showed excellent colloidal-stability and intense fluorescence in various aqueous solutions as compared to pristine GO and the GO covalently functionalized with dextran. The fluorescence of PhO-dex-GO remarkably increased as AChE catalyzed the hydrolysis of acetylthiocholine (ATCh) to give thiocholine and acetic acid. It was found that the turn-on fluorescence response of PhO-dex-GO to AChE activity was induced by protonation of carboxyl groups on it from the product of the enzymatic hydrolysis reaction, acetic acid. Based on its turn-on fluorescence response, PhO-dex-GO was able to report kinetic and thermodynamic parameters involving a maximum velocity, a Michaelis constant and

an inhibition dissociation constant for AChE activity and inhibition. These parameters enable us to determine the activity of AChE and the efficiency of the inhibitor.

Keywords: acetylcholinesterase, graphene oxide, GO fluorescence, inhibitor detection, optical biosensor.

Alzheimer's disease (AD)[1, 2] is a chronic and degenerative cognitive disorder, and is a leading cause of dementia in elderly people. AD is believed to be caused by the self-assembling of amyloid beta (Aβ) peptides, producing fibrillar Aβ oligomers that accumulate in the brain;[3] this process can be induced by acetylcholinesterase (AChE) catalyzing the hydrolysis of acetylcholine (ACh) to yield choline and acetic acid.[4-6] Hence, the inhibition of AChE activity is considered a promising clinical treatment to delay onset of AD and improve AD symptoms.[7, 8] In order to monitor the activity of AChE and its inhibition, several assay methods have been developed. The conventional assay for AChE activity is based on the reaction of thiols with 5,5'-dithiobis-(2-nitrobenzoic acid) to give 2-nitro-5-thiobenzoate which is quantified by measuring its absorbance at 412 nm.[9] However, this conventional method shows low sensitivity. Another method widely used for assessing AChE activity and its inhibition rests on an enzyme cascade reaction using an additional enzyme such as horseradish peroxidase (HRP) or choline oxidase in addition to AChE.[10-14] This cascade assay involves multi-step procedures and extra enzymes,

rendering it complex and time-consuming. Moreover, this enzyme cascade assay might not be suitable for the precise kinetic measurement of AChE activity and its inhibition, since the hydrogen peroxide produced by additional enzymes, and not by AChE, leads to the response signals in the assay. Recently, continuous fluorescent assays for the direct measurement of AChE activity have been reported;[15, 16] however, the additional modification of the substrate ACh with a quencher is essential to the process. Therefore, it is still required to develop a simple and effective assay platform capable of reporting the direct reaction kinetics for AChE activity and its inhibition.

Graphene oxide (GO) is an oxidized form of graphene involving various oxygen-containing functional groups.[17-19] A disruption of conjugated π-bonds *via* oxidation in GO opens an electronic band gap due to quantum confinement or intervalley scattering, resulting in the emission of strong and tunable fluorescence in the visible and near infrared region of the electromagnetic spectrum.[20-22] It has been found that the fluorescence of GO is significantly more stable with respect to photobleaching when compared to organic fluorescent dyes.[23] Due to its beneficial photophysical properties, GO fluorescence has been exploited as a sensing tool for the detection of biological molecules,[24-27] though it remains at an early stage. Hence, it is of great interest to develop GO fluorescence-based optical biosensors as alternatives to address the deficiencies of conventional bioassays. For the use of GO fluorescence as a signal transduction tool in bioassays, it is essential to functionalize GO in order to retain its intense fluorescence emission and colloidal stability during the entire reaction period. In particular, a non-covalent approach which retains oxygen-containing functional groups on the GO is required, since these affect GO's intense fluorescence emission and fluorescence response to target molecules.[26, 28]

Herein, we demonstrate an optical biosensor based on fluorescence exhibited by GO non-covalently functionalized with phenoxy-modified dextran (denoted "PhO-dex-GO") for the detection of AChE activity and its inhibitors. The fluorescence properties and colloidal stability of PhO-dex-GO were investigated, and compared to those of pristine GO and the GO that was covalently functionalized with dextran (denoted "dex-GO"). PhO-dex-GO exhibiting intense fluorescence and outstanding colloidal stability in aqueous solutions was then applied to the detection of hydrolysis activity of AChE and its inhibition, providing kinetic and thermodynamic parameters such as a maximum velocity (v_{max}), a Michaelis constant (K_m), and an inhibition dissociation constant (K_d). In addition, we explored a mechanism responsible for the fluorescence response of PhO-dex-GO to the enzymatic hydrolysis of acetylthiocholine (ATCh) and AChE inhibition.

RESULTS AND DISCUSSION

The principle of the PhO-dex-GO sensor for the detection of AChE activity and inhibitors is depicted in Figure 1. In the presence of AChE, the substrate ATCh underwent enzymatic hydrolysis to produce thiocholine and acetic acid, resulting in a fluorescence increase on PhO-dex-GO.

To design PhO-dex-GO, graphite oxide was prepared *via* a modified Hummers method.[17] As-prepared graphite oxide was then dispersed *via* a synthetic polymer, phenoxy dextran (PhO-dex),[29, 30] bearing a hydrophobic group in water through ultra-sonication in an ice bath for 30 min. After centrifugation at 10,000 rpm for 15 min, the supernatant, including the GO non-covalently functionalized with PhO-dex (PhO-dex-GO, 0.46 mg/mL), was obtained. The hydrophobic

interaction of the phenoxy groups in PhO-dex with the hydrophobic plane of conjugated π-bonds in GO produced a stable complex of PhO-dex-GO in aqueous solution. For comparison, GO was covalently functionalized with dextran (dex-GO) in the presence of ammonium hydroxide (Method in Supporting Information). PhO-dex-GO and dex-GO were then analyzed using atomic force microscopy (AFM), as shown in Figure 2 and Figure S1. PhO-dex-GO exhibits a sheet structure with a lateral size of 200-500 nm (Figure 2a). It was found that its height increased to *ca*. 2.3 nm (Figure 2b) over that of pristine GO (*ca*. 1 nm, Figure S1a), indicating that PhO-dex was introduced on the surface of the GO. The height of dex-GO also increased to *ca*. 2.0 nm, as shown in Figure S1b.

After washing free PhO-dex polymers from the PhO-dex-GO solution using a centrifugal filter device, PhO-dex-GO was dried for Fourier transform infrared (FT-IR) spectroscopy analysis. Figure 2c shows the characteristic vibrational modes for PhO-dex adsorbed on GO in the spectrum of PhO-dex-GO (red line). The bending modes for the C−O−H and C−O−C bonds in the dextran backbone of PhO-dex clearly appeared at 1016, 1041, 1076, 1112, and 1147 cm^{-1}.[31, 32] In addition, the stretching mode for the sp^2 C−O bond in a phenoxy group was observed at 1246 cm^{-1}. Note that the characteristic stretching modes for C=O, C−O, and C−O−C bonds in pristine GO were still clearly observed in PhO-dex-GO, indicating that functional groups such as the carboxyl, hydroxyl, and epoxide groups remain the same as in GO. An electronic transition from the π to π* orbital in the phenoxy groups was also observed in the ultraviolet (UV) spectrum of PhO-dex-GO (Figure 2d). These analytical results suggest that PhO-dex-GO was successfully prepared through the non-covalent dispersion of graphite oxide using PhO-dex. The covalently functionalized GO (dex-GO) was also analyzed using FT-IR and UV spectroscopy (Figure S2). The characteristic peaks for dextran at 1016, 1041, 1076, 1107, and 1147 cm^{-1} were

also observed in the FT-IR spectrum of the dex-GO as in the PhO-dex-GO; however, the peak intensity at 1734 and 1261 cm^{-1} responsible for C=O and C−O−C stretching in the carboxyl and epoxide groups of GO significantly decreased in the spectrum of dex-GO, indicating that the oxygen-containing functional groups on pristine GO were damaged during covalent functionalization. This spectroscopic analysis shows that dex-GO was prepared as well.

Following the FT-IR analysis, the fluorescence property and the colloidal stability of PhO-dex-GO, dex-GO, and pristine GO were investigated in 4-(2-hydroxyethyl)-1-piperazine-ethanesulfonic acid (HEPES) buffer solution (pH 8.0, 5 mM) in which AChE activity is commonly assessed. As shown in Figure 3a, the fluorescence emission of PhO-dex-GO (50 μg/mL) was intense in buffer solution (red line), and was slightly higher than that of pristine GO (black line). The spectral shape of PhO-dex-GO was almost identical to that of pristine GO; however, the covalently functionalized dex-GO at the same concentration showed a significantly reduced intensity of fluorescence emission (blue line) as compared to PhO-dex-GO and pristine GO. This significant reduction in the fluorescence of dex-GO can be attributed to damage to the C=O and C−O functional groups in GO during covalent functionalization, as shown in the FT-IR spectrum in Figure S2a. This damage results in a diminution in the electronic transitions between the confined C=C cluster and the boundary of the oxidized region.[33] It has been reported that the carbonyl functional groups in GO contribute to this long wavelength emission.[28, 34] These results suggest that a non-covalent approach to the functionalization of GO is significantly more beneficial than a covalent approach in terms of optical property. Due to the weak fluorescence of dex-GO, it was not examined farther in other solvent systems. The fluorescence of PhO-dex-GO and pristine GO was then measured under various medium conditions (water, buffer, and ATCh-containing solutions. Figure 3b shows a 50 % reduction in GO fluorescence in HEPES buffer

solution, while PhO-dex-GO still exhibited very intense fluorescence with minimal change (Figure 3c) as compared to that in water. In addition, when ATCh (19 mM) was added as a substrate to a HEPES buffer solution of GO, it was found that its fluorescence was more significantly diminished (Figure 3b, blue line), while PhO-dex-GO continued to emit fluorescence at an intensity similar to that observed in water and a HEPES solution (Figure 3c, blue line).

In order to understand the dramatic decrease in GO fluorescence under the ATCh and HEPES buffer solutions, we measured the size distribution of GO and PhO-dex-GO using dynamic light scattering (DLS). As shown in Figure 3d, the size distribution of GO in a HEPES buffer solution shifted towards the right, and this shifting was more noticeable in an ATCh solution. According to the results of DLS analysis, the average size of the GO gradually increased from 133, to 242, to 728 nm in water, a HEPES solution, and an ATCh solution, respectively. This result indicates that GO underwent aggregation due to low colloidal stability in the solutions with high ionic strength or a high concentration of enzyme substrate, which resulted in a significant diminution of fluorescence emission. The aggregated GO in ATCh solution was macroscopically observed without magnification (inset: optical image), while PhO-dex-GO showed outstanding colloidal stability in all different solutions. The size distribution of PhO-dex-GO appeared similar in three different cases (from 178 to 179 nm in average size). On the basis of colloidal and optical stability, we expect that the non-covalently functionalized PhO-dex-GO can be properly applied to the detection of AChE activity and inhibitors.

We then investigated the fluorescence response of PhO-dex-GO to the enzymatic hydrolysis of ATCh in the presence of AChE in HEPES buffer solution (pH 8.0, 5 mM). During this process, ATCh is hydrolyzed by the enzyme into thiocholine and acetic acid. One of the products in the

enzyme reaction, acetic acid, provides the PhO-dex-GO with acidic protons for protonation of the carboxyl groups in PhO-dex-GO, which could lead to a change in its fluorescence. We measured the fluorescence of PhO-dex-GO by varying the concentration of the enzyme AChE from 0.95 to 2.38 U/mL at a constant concentration of ATCh (19 mM). The fluorescence was measured 15 min after incubation of the mixture at 37 ºC. Figure 4a, 4b, and S3 show that the fluorescence of PhO-dex-GO increased with increasing the concentrations of AChE. No fluorescence increase was observed as the enzyme (AChE) was added alone to the solution of PhO-dex-GO in the absence of ATCh (Figure S4). In order to confirm that ATCh underwent enzymatic hydrolysis, the production of thiocholine was monitored using Ellman's method, in which 5,5'-dithiobis-(2-nitrobenzoic acid) is converted into 2-nitro-5-thiobenzoate, which is quantified by measuring an absorbance at 412 nm.[9] As shown in Figure 4c, the absorbance at 412 nm gradually increased with increasing the concentrations of AChE, indicating that the enzymatic hydrolysis of ATCh occurred in the PhO-dex-GO solution and proceeded more rapidly at higher enzyme concentrations. The extent of enzymatic hydrolysis was in good agreement with the fluorescence increase of PhO-dex-GO. Then, we measured the pH values of the solution after the enzymatic hydrolysis reaction. As shown in Figure S5, the pH value of the solution decreased as a function of AChE concentrations. The production of acetic acid can be accelerated at higher concentrations of AChE, leading to a larger decrease in the pH of the solution. This pH decrease can lead to protonation in the PhO-dex-GO carboxyl groups, resulting in increased fluorescence. Figure 4d shows that the fluorescence intensity of the PhO-dex-GO increased as the solution pH decreased. This pH effect on the fluorescence of PhO-dex-GO is consistent with previously-reported results.[35, 36]

Next, we varied the concentration of ATCh from 2.38 to 28.5 mM at a constant concentration of AChE (1.9 U/mL) in HEPES buffer solution (pH 8.0, 5 mM) to examine the fluorescence response of PhO-dex-GO. As shown in Figure 5a and S6, the fluorescence of PhO-dex-GO increased with increasing concentrations of ATCh; however, no fluorescence change was observed as ATCh was added alone without the enzyme AChE (Figure S7). In addition, PhO-dex-GO continued to be stably dispersed without aggregation during the entire period of reaction (Figure S8). These results indicate that the fluorescence increase in PhO-dex-GO was a result of the enzymatic hydrolysis of ATCh which produces acidic protons. The hydrolysis of ATCh was confirmed *via* Ellman's method again, and Figure 5b shows that the absorbance at 412 nm increased as a function of ATCh concentrations, indicating that ATCh was effectively converted into thiocholine and acetic acid by AChE. We plotted the fluorescence response of PhO-dex-GO and the pH value of the reaction solution against the concentration of ATCh (Figure 5c). It can be clearly observed that the fluorescence of PhO-dex-GO increased (black squares) as the pH value of the solution decreased gradually from 7.8 to 5.5 (red inverted triangles) as a function of ATCh concentrations. In order to measure the enzyme reaction kinetics based on the turn-on fluorescence response of PhO-dex-GO, the fluorescence response rates were measured at the early stage of the enzyme reactions within 2 min at 37 ºC (details in Supporting Information). Then, a plot of reciprocal fluorescence response rates with reciprocal ATCh concentrations was obtained, which obeys the Lineweaver-Burk equation (Figure 5d). This plot yielded a Michaelis constant (K_m) of 0.494 mM and a maximum velocity (v_{max}) of 0.083 min^{-1}, respectively, which are similar to those previously reported.[9, 37] This result shows that PhO-dex-GO was able to report the information about the reaction kinetics of AChE activity based on its turn-on fluorescence response. During kinetics measurement of AChE activity, the pH value of the PhO-

dex-GO solution decreased from 7.8 to 7.0 along with its fluorescence increase (Figure S9). It was found that the activity of AChE remained almost same in this pH range when it was assessed by Ellman's reagent (Figure S10). This pH dependency of AChE activity is also in good agreement with the previous result reported in other literature.[38]

In order to investigate the sensitivity of PhO-dex-GO for detection of AChE activity, the concentration of AChE was varied from 0.1 to 100 mU/mL in the presence of ATCh (19 mM). As shown in Figure S11, the fluorescence of PhO-dex-GO gradually increased with increasing the AChE concentration from 0.1 to 100 mU/mL. The limit of detection (LOD) was calculated based on the standard deviation of the response (SD) and the slope of the calibration curve (S) at levels approximating the LOD according to the formula: LOD = 3.3(SD/S). LOD of PhO-dex-GO for AChE activity was found to be 0.27 mU/mL. We also examined LOD of Ellman's method in the same concentration range of AChE (Figure S12). LOD of Ellman's method for AChE activity was found to be 1.26 mU/mL, which is very similar to the value reported in other literature. These results clearly suggest that PhO-dex-GO is more sensitive to detection of AChE activity than the conventional assay, Ellman's method.

After then, we further examined whether PhO-dex-GO can detect an AChE inhibitor. Paraoxon[39, 40], which is known as an irreversible inhibitor, was chosen as a model inhibitor to AChE. In inhibition assay, paraoxon at various concentrations was incubated first with AChE (1.9 U/mL) for 5 min at 37 ºC, and the resulting solution was added to the PhO-dex-GO solution containing 19 mM of ATCh. After additional incubation for 15 min at 37 ºC, the fluorescence of PhO-dex-GO was measured. As shown in Figure 6a, the increased fluorescence in PhO-dex-GO was clearly observed in the absence of paraoxon. However, its turn-on fluorescence response was gradually reduced as the concentration of paraoxon increased in the solution. We calculated

LOD of the PhO-dex-GO sensor for the inhibitor in the same way as LOD for detection of AChE activity was determined. We found that its LOD was 28.55 nM, which is comparable to values reported based on other methods.[41] In the control experiments, only paraoxon or mixtures of paraoxon and AChE were added into the PhO-dex-GO solution in the absence of ATCh, but no fluorescence change was observed (Figure S13). We carried out additional control experiments to demonstrate the selective screening of the inhibitor to AChE using PhO-dex-GO. Thiram, which is known to inhibit the activity of glutathione reductase,[42] was examined as a negative control. As shown in Figure S14, the turn-on fluorescence response in PhO-dex-GO was still observed in the presence of thiram at all concentrations, indicating that it was not able to inhibit the activity of AChE. This result clearly suggests that PhO-dex-GO was able to selectively detect an inhibitor to AChE.

In order to determine the inhibition efficiency of paraoxon, the kinetics of AChE inhibition with paraoxon at various concentrations was measured through the fluorescence changes of PhO-dex-GO against time (Figure S15). Then, a Zero-Time method[43] was applied to the plots to obtain the initial velocity of reaction at zero time for each concentration of paraoxon, followed by calculation of extract its dissociation constant (K_d) as shown below. The initial velocity of reaction at zero time can be obtained on the basis of the fluorescence response rate of PhO-dex-GO at each concentration of paraoxon.

The equation of Zero-Time method is shown below;

$$K_d = \frac{K_m[P]}{(K_m + [S])(\frac{v_c}{v_0} - 1)} \qquad (1)$$

Where K_d is a dissociation constant, K_m is the Michaelis constant of AChE, [P] is the concentration of paraoxon, [S] is the concentration of ATCh, v_o is the initial velocity of reaction based on the fluorescence response rates in the presence of paraoxon at a certain concentration, and v_c is the velocity of reaction based on the fluorescence response rates in the absence of paraoxon.

As shown in Figure 6b, the Zero-Time plots of reaction velocities appeared to be linear, so the initial velocity of reaction at zero time (v_o) for each concentration of paraoxon was obtained *via* extrapolation of the plots using the least squares method (0.00135, 0.00131, and 0.00126 sec^{-1}). Then, the mean value of K_d (0.856 ± 0.073 μM) was calculated by substitution of these values into the equation (1). This obtained value of K_d of paraoxon for AChE inhibition was found to be similar with that previously reported in the literature.[44] This result suggests that the non-covalently functionalized PhO-dex-GO is a versatile optical sensor for determining the inhibition efficiency based on inhibition kinetics as well as the reaction kinetics for AChE activity.

CONCLUSIONS

We have developed the PhO-dex-GO platform by functionalizing GO non-covalently with PhO-dex for the measurement of AChE activity and inhibitors based on its turn-on fluorescence response. The non-covalently functionalized PhO-dex-GO exhibits excellent colloidal stability and intense fluorescence in various aqueous solutions, and is able to detect the activity of AChE and its inhibitor in a simple and rapid manner. In addition, PhO-dex-GO was able to provide kinetic and thermodynamic parameters in relation to AChE activity and inhibition, enabling determination of AChE activity and the efficiency of an inhibitor. We expect that this PhO-dex-

GO platform could be extended to high-throughput screening of AChE inhibitors for treatment of Alzheimer's disease.

EXPERIMENTAL METHOD

Materials

Graphite flakes, sodium nitrate, potassium permanganate, sodium hydroxide, dextran (10 kDa), 1,2-epoxy-3-phenoxypropane, Acetylcholinesterase from Electrophorus electricus (electric eel) (AChE), acetylthiocholine (ATCh), paraoxon-ethyl, 5,5`-dithiobis(2-nitrobenzoic acid) (DTNB), and 4-(2-hydroxyethyl)-1-piperazine-ethanesulfonic acid (HEPES) were purchased from Sigma Aldrich. Sulfuric Acid, hydrogen peroxide, and hydrogen chloride were purchased from Daejung, Korea.

Synthesis of PhO-dex-GO

To synthesize PhO-dex, a 1 g portion of dextran (10 kDa) was dissolved in 1 M of NaOH solution (10 mL), followed by the addition of 0.75 mL of 1,2-epoxy-3-phenoxypropane in an ice bath.[29, 30] After stirring the mixture for 10 h at 40 ºC, a 150 mL portion of methanol was slowly added into the reaction mixture to precipitate the desired product (PhO-dex). The precipitated product was then washed with methanol several times, and was dried under vacuum.

Graphite oxide was synthesized *via* a modified Hummers method.[17] 17 mL of H_2SO_4, 375 mgs of $NaNO_3$ and 0.5 g of graphite were added into a round-bottom flask. A 2.5 g portion of $KMnO_4$ was slowly added into the graphite solution, and the temperature increased to 35 ºC. The reaction mixture was stirred for an additional 2 h, followed by the slow addition of water (30 mL) in an

ice bath. After stirring the resulting mixture for 2 h at room temperature, a 2 mL portion of H_2O_2 was added to the solution in an ice bath, and stirred for 30 min. After the addition of HCl solution (10 v/v %), graphite oxide was centrifuged and washed extensively with water. After neutralizing the graphite oxide solution with 0.1 M of NaOH solution, it was washed with water and dried under vacuum.

A 15 mg portion of graphite oxide and a 15 mg portion of PhO-dex were added to 15 mL of water, which was then sonicated for 30 min in an ice bath. The resulting solution was centrifuged at 10,000 rpm for 15 min, and the supernatant was collected and used for further experiment.

General procedure for the measurement of AChE activity and its inhibitor with PhO-dex-GO

In order to detect AChE activity based on fluorescence response, PhO-dex-GO (200 μg) was dispersed in 4 mL of HEPES buffer solution (5 mM, pH 8.0). A 400 μL aliquot of PhO-dex-GO was added to a microtube in which a 10 μL portion of AChE and a 10 μL portion of ATCh were added at the desired concentration. The mixture was shaken for 15 min at 37 ºC. The fluorescence of PhO-dex-GO was then measured *via* excitation at 445 nm and acquisition for 0.05 sec. Fitting was done with instrumental weighting method; $\omega_i = 1/\sigma_i^2$, which σ_i^2 are the error bar sizes stored in error bar columns.

To perform an assay for the detection of an inhibitor with PhO-dex-GO, 10 μL of AChE (80 U/mL) was mixed with a 10 μL portion of paraoxon (16 μM), and the resulting mixture was incubated for 5 min at 37 ºC. The AChE/paraoxon solution was added to a 400 μL portion of phO-dex-GO (50 μg/mL, HEPES buffer, pH 8.0) containing ATCh (19 mM), and the resulting

mixture was shaken for 15 min at 37 ºC. Then the fluorescence of PhO-dex-GO was measured with excitation at 445 nm and acquisition for 0.05 sec.

ASSOCIATED CONTENT

Supporting Information

Instruments, additional experimental methods and data for GO and dex-GO, the fluorescence responses without AChE or ATCh, and the fluorescence responses to thiram *etc*. This material is available free of charge *via* the Internet at http://pubs.acs.org.

ACKNOWLEDGEMENT

This work was supported by the Basic Science Research Program (NRF-2014R1A2A1A11051877 and 2008-0061891), and the Pioneer Research Center Program (NRF-2011-0021021) through the National Research Foundation of Korea (NRF) funded by the Ministry of Science, ICT and Future Planning.

REFERENCES

1. Khachaturian, Z. S. Diagnosis of Alzheimers Disease. *Arch. Neurol. (Chicago)* 1985, 42, 1097-1104.
2. Jack, C. R.; Lowe, V. J.; Weigand, S. D.; Wiste, H. J.; Senjem, M. L.; Knopman, D. S.; Shiung, M. M.; Gunter, J. L.; Boeve, B. F.; Kemp, B. J.; Weiner, M.; Petersen, R. C.; Initi, A. s. D. N. Serial PIB and MRI in Normal, Mild Cognitive Impairment and Alzheimer`s Disease: Implications for Sequence of Pathological Events in Alzheimers Disease. *Brain* 2009, 132, 1355-1365.
3. Rushworth, J. V.; Griffiths, H. H.; Watt, N. T.; Hooper, N. M. Prion Protein-Mediated Toxicity of Amyloid-β Oligomers Requires Lipid Rafts and the Transmembrane LRP1. *J. Biol. Chem.* 2013, 288, 8935-8951.
4. Inestrosa, N. C.; Alvarez, A.; Perez, C. A.; Moreno, R. D.; Vicente, M.; Linker, C.; Casanueva, O. I.; Soto, C.; Garrido, J. Acetylcholinesterase Accelerates Assembly of Amyloid-

β-Peptides into Alzheimer's Fibrils: Possible Role of the Peripheral Site of the Enzyme. *Neuron* 1996, 16, 881-891.
5. Bartolini, M.; Bertucci, C.; Cavrini, V.; Andrisano, V. β-Amyloid Aggregation Induced by Human Acetylcholinesterase: Inhibition Studies. *Biochem Pharmacol* 2003, 65, 407-416.
6. Talesa, V. N. Acetylcholinesterase in Alzheimer's Disease. *Mech. Ageing Dev.* 2001, 122, 1961-1969.
7. Ellis, J. M. Cholinesterase Inhibitors in the Treatment of Dementia. *J. Am. Osteopath. Assoc.* 2005, 105, 145-158.
8. Rozzini, L.; Costardi, D.; Chilovi, B. V.; Franzoni, S.; Trabucchi, M.; Padovani, A. Efficacy of Cognitive Rehabilitation in Patients with Mild Cognitive Impairment Treated with Cholinesterase Inhibitors. *Int. J. Geriatr. Psychopharmacol.* 2007, 22, 356-360.
9. Ellman, G. L.; Courtney, K. D.; Andres, V.; Featherstone, R. M. A New and Rapid Colorimetric Determination of Acetylcholinesterase Activity. *Biochem. Pharmacol.* 1961, 7, 88-95.
10. Gill, R.; Bahshi, L.; Freeman, R.; Willner, I. Optical Detection of Glucose and Acetylcholine Esterase Inhibitors by H2O2-Sensitive CdSe/ZnS Quantum Dots. *Angew. Chem. Int. Ed.* 2008, 47, 1676-1679.
11. Wang, J.; Suzuki, H.; Satake, T. Coulometric Microdevice for Organophosphate Pesticide Detection. *Sens. Actuators, B* 2014, 204, 297-301.
12. Hadd, A. G.; Jacobson, S. C.; Ramsey, J. M. Microfluidic Assays of Acetylcholinesterase Inhibitors. *Anal. Chem.* 1999, 71, 5206-5212.
13. Guardigli, M.; Pasini, P.; Mirasoli, M.; Leoni, A.; Andreani, A.; Roda, A. Chemiluminescent High-Throughput Microassay for Evaluation of Acetylcholinesterase Inhibitors. *Anal. Chim. Acta* 2005, 535, 139-144.
14. Pavlov, V.; Xiao, Y.; Willner, I. Inhibition of the Acetycholine Esterase-Stimulated Growth of Au Nanoparticles: Nanotechnology-Based Sensing of Nerve Gases. *Nano Lett.* 2005, 5, 649-653.
15. Feng, F. D.; Tang, Y. L.; Wang, S.; Li, Y. L.; Zhu, D. B. Continuous Fluorometric Assays for Acetylcholinesterase Activity and Inhibition with Conjugated Polyelectrolytes. *Angew. Chem. Int. Ed.* 2007, 46, 7882-7886.
16. Shen, X.; Liang, F. X.; Zhang, G. X.; Zhang, D. Q. A New Continuous Fluorometric Assay for Acetylcholinesterase Activity and Inhibitor Screening with Emissive Core-Shell Silica Particles Containing Tetraphenylethylene Fluorophore. *Analyst* 2012, 137, 2119-2123.
17. Hummers, W. S.; Offeman, R. E. Preparation of Graphitic Oxide. *J. Am. Chem. Soc.* 1958, 80, 1339-1339.
18. Dreyer, D. R.; Park, S.; Bielawski, C. W.; Ruoff, R. S. The Chemistry of Graphene Oxide. *Chem. Soc. Rev.* 2010, 39, 228-240.
19. Chen, D.; Feng, H. B.; Li, J. H. Graphene Oxide: Preparation, Functionalization, and Electrochemical Applications. *Chem. Rev.* 2012, 112, 6027-6053.
20. Luo, Z. T.; Vora, P. M.; Mele, E. J.; Johnson, A. T. C.; Kikkawa, J. M. Photoluminescence and Band Gap Modulation in Graphene Oxide. *Appl. Phys. Lett.* 2009, 94, 111909.
21. Sun, X. M.; Liu, Z.; Welsher, K.; Robinson, J. T.; Goodwin, A.; Zaric, S.; Dai, H. J. Nano-Graphene Oxide for Cellular Imaging and Drug Delivery. *Nano Res.* 2008, 1, 203-212.
22. Chien, C. T.; Li, S. S.; Lai, W. J.; Yeh, Y. C.; Chen, H. A.; Chen, I. S.; Chen, L. C.; Chen, K. H.; Nemoto, T.; Isoda, S.; Chen, M. W.; Fujita, T.; Eda, G.; Yamaguchi, H.; Chhowalla, M.;

Chen, C. W. Tunable Photoluminescence from Graphene Oxide. *Angew. Chem. Int. Ed.* 2012, 51, 6662-6666.
23. Roy, M.; Kusurkar, T. S.; Maurya, S. K.; Meena, S. K.; Singh, S. K.; Sethy, N.; Bhargava, K.; Sharma, R. K.; Goswami, D.; Sarkar, S.; Das, M. Graphene Oxide from Silk Cocoon: a Novel Magnetic Fluorophore for Multi-Photon Imaging. *3 Biotech* 2014, 4, 67-75.
24. Jung, J. H.; Cheon, D. S.; Liu, F.; Lee, K. B.; Seo, T. S. A Graphene Oxide Based Immuno-Biosensor for Pathogen Detection. *Angew. Chem. Int. Ed.* 2010, 49, 5708-5711.
25. Chen, J. L.; Yan, X. P.; Meng, K.; Wang, S. F. Graphene Oxide Based Photoinduced Charge Transfer Label-Free Near-Infrared Fluorescent Biosensor for Dopamine. *Anal. Chem.* 2011, 83, 8787-8793.
26. Jeon, S. J.; Kwak, S. Y.; Yim, D.; Ju, J. M.; Kim, J. H. Chemically-Modulated Photoluminescence of Graphene Oxide for Selective Detection of Neurotransmitter by "Turn-On" Response. *J. Am. Chem. Soc.* 2014, 136, 10842-10845.
27. Kwak, S. Y.; Yang, J. K.; Jeon, S. J.; Kim, H. I.; Yim, J.; Kang, H.; Kyeong, S.; Lee, Y. S.; Kim, J. H. Luminescent Graphene Oxide with a Peptide-Quencher Complex for Optical Detection of Cell-Secreted Proteases by a Turn-On Response. *Adv. Funct. Mater.* 2014, 24, 5119-5128.
28. Cushing, S. K.; Li, M.; Huang, F. Q.; Wu, N. Q. Origin of Strong Excitation Wavelength Dependent Fluorescence of Graphene Oxide. *ACS Nano* 2014, 8, 1002-1013.
29. Barone, P. W.; Strano, M. S. Reversible Control of Carbon Nanotube Aggregation for a Glucose Affinity Sensor. *Angew. Chem. Int. Ed.* 2006, 45, 8138-8141.
30. Kim, H. I.; Hwang, D.; Jeon, S. J.; Lee, S.; Park, J. H.; Yim, D.; Yang, J. K.; Kang, H.; Choo, J.; Lee, Y. S.; Chung, J.; Kim, J. H. Orientation and Density Control of Bispecific Anti-HER2 Antibody on Functionalized Carbon Nanotubes for Amplifying Effective Binding Reactivity to Cancer Cells. *Nanoscale* 2015, 7, 6363-6373.
31. Cao, W.; Li, X. Q.; Liu, L.; Yang, T. H.; Li, C.; Fan, H. T.; Jia, M.; Lv, Z. G.; Mei, Q. B. Structure of an Anti-Tumor Polysaccharide from Angelica Sinensis (Oliv.) Diels. *Carbohydr. Polym.* 2006, 66, 149-159.
32. Khot, V. M.; Salunkhe, A. B.; Thorat, N. D.; Ningthoujam, R. S.; Pawar, S. H. Induction Heating Studies of Dextran Coated MgFe2O4 Nanoparticles for Magnetic Hyperthermia. *Dalton Trans.* 2013, 42, 1249-1258.
33. Shang, J. Z.; Ma, L.; Li, J. W.; Ai, W.; Yu, T.; Gurzadyan, G. G. The Origin of Fluorescence from Graphene Oxide. *Sci. Rep.* 2012, 2, 792.
34. Li, M.; Cushing, S. K.; Zhou, X. J.; Guo, S. W.; Wu, N. Q. Fingerprinting Photoluminescence of Functional Groups in Graphene Oxide. *J. Mater. Chem.* 2012, 22, 23374-23379.
35. Galande, C.; Mohite, A. D.; Naumov, A. V.; Gao, W.; Ci, L. J.; Ajayan, A.; Gao, H.; Srivastava, A.; Weisman, R. B.; Ajayan, P. M. Quasi-Molecular Fluorescence from Graphene Oxide. *Sci. Rep.* 2011, 1, 85.
36. Chen, J. L.; Yan, X. P. Ionic Strength and pH Reversible Response of Visible and Near-Infrared Fluorescence of Graphene Oxide Nanosheets for Monitoring the Extracellular pH. *Chem. Commun.* 2011, 47, 3135-3137.
37. Arduini, F.; Guidone, S.; Amine, A.; Palleschi, G.; Moscone, D. Acetylcholinesterase Biosensor Based on Self-Assembled Monolayer-Modified Gold-Screen Printed Electrodes for Organophosphorus Insecticide Detection. *Sens. Actuators, B* 2013, 179, 201-208.

38. Moradzadegan, A.; Ranaei-Siadat, S. O.; Ebrahim-Habibi, A.; Barshan-Tashnizi, M.; Jalili, R.; Torabi, S. F.; Khajeh, K. Immobilization of Acetylcholinesterase in Nanofibrous PVA/BSA Membranes by Electrospinning. *Eng. Life Sci.* 2010, 10, 57-64.
39. Zejli, H.; de Cisneros, J. L. H. H.; Naranjo-Rodriguez, I.; Liu, B. H.; Temsamani, K. R.; Marty, J. L. Alumina Sol-Gel/Sonogel-Carbon Electrode Based on Acetylcholinesterase for Detection of Organophosphorus Pesticides. *Talanta* 2008, 77, 217-221.
40. Chen, H. D.; Zuo, X. L.; Su, S.; Tang, Z. Z.; Wu, A. B.; Song, S. P.; Zhang, D. B.; Fan, C. H. An Electrochemical Sensor for Pesticide Assays Based on Carbon Nanotube-Enhanced Acetycholinesterase Activity. *Analyst* 2008, 133, 1182-1186.
41. Dhull, V.; Gahlaut, A.; Dilbaghi, N.; Hooda, V. Acetylcholinesterase Biosensors for Electrochemical Detection of Organophosphorus Compounds: a Review. *Biochem. Res. Int.* 2013, 2013, 731501.
42. Cereser, C.; Boget, S.; Parvaz, P.; Revol, A. Thiram-Induced Cytotoxicity is Accompanied by a Rapid and Drastic Oxidation of Reduced Glutathione with Consecutive Lipid Peroxidation and Cell Death. *Toxicology* 2001, 163, 153-162.
43. Gray, P. J.; Duggleby, R. G. Analysis of Kinetic Data for Irreversible Enzyme-Inhibition. *Biochem. J* 1989, 257, 419-424.
44. Milatovic, D.; Dettbarn, W. D. Modification of Acetylcholinesterase During Adaptation to Chronic, Subacute Paraoxon Application in Rat. *Toxicol. Appl. Pharmacol.* 1996, 136, 20-28.

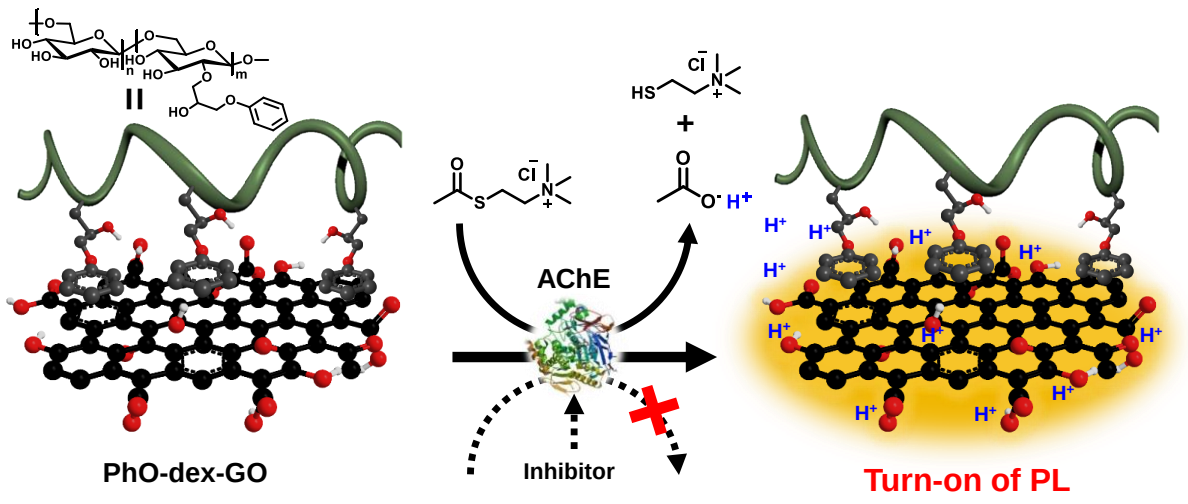

Figure 1. Schematic illustration for the detection of acetylcholinesterase (AChE) activity and inhibitors through the fluorescence response of phenoxy dextran-functionalized GO (PhO-dex-GO).

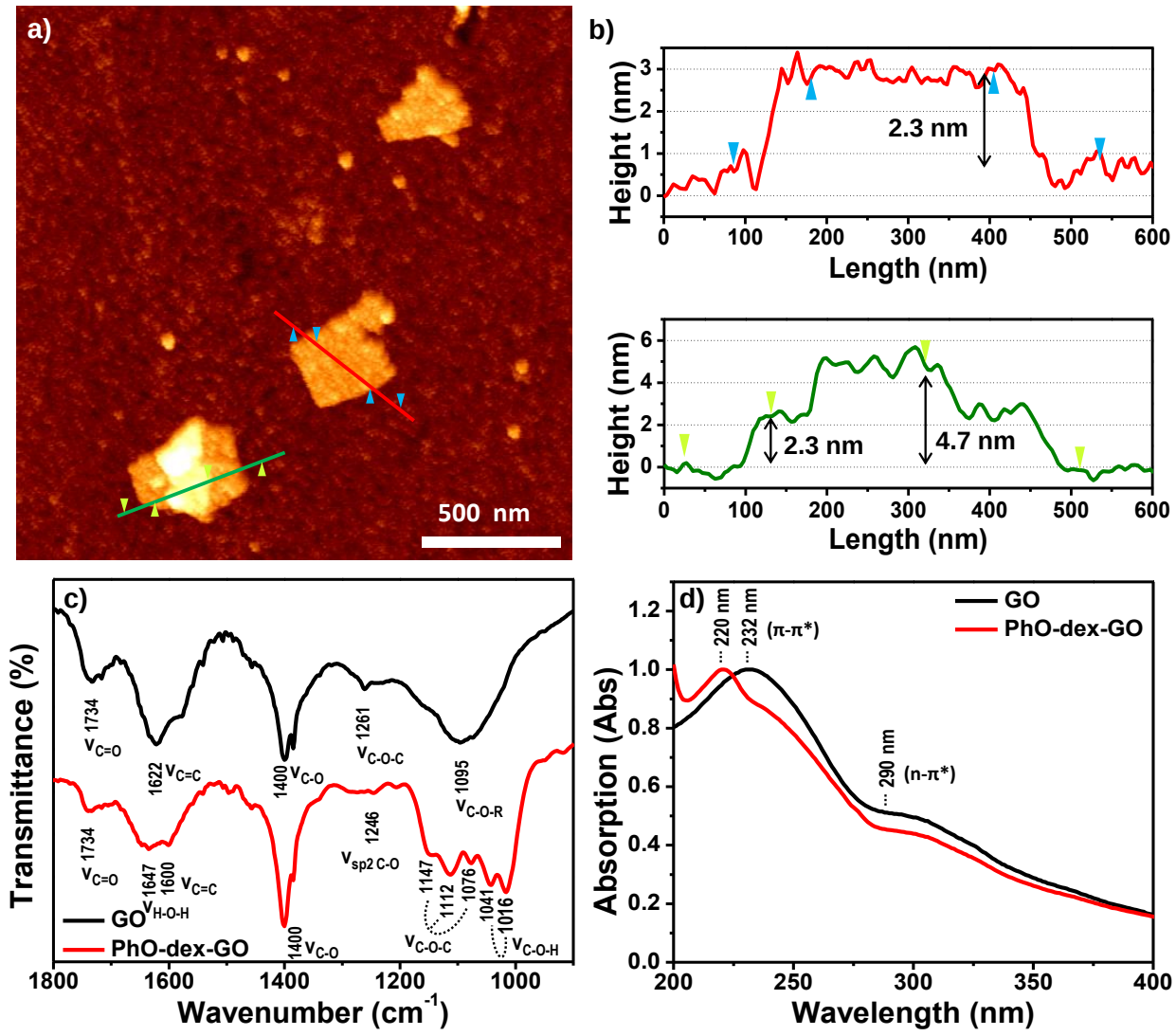

Figure 2. Characterization of non-covalently functionalized PhO-dex-GO. (a) AFM image of PhO-dex-GO and b) its height profiles, showing a height increase from 1.0 to 2.3 nm as compared to pristine GO. c) FT-IR spectra and d) UV absorption spectra showing the clear vibrational and absorption features of PhO-dex and GO.

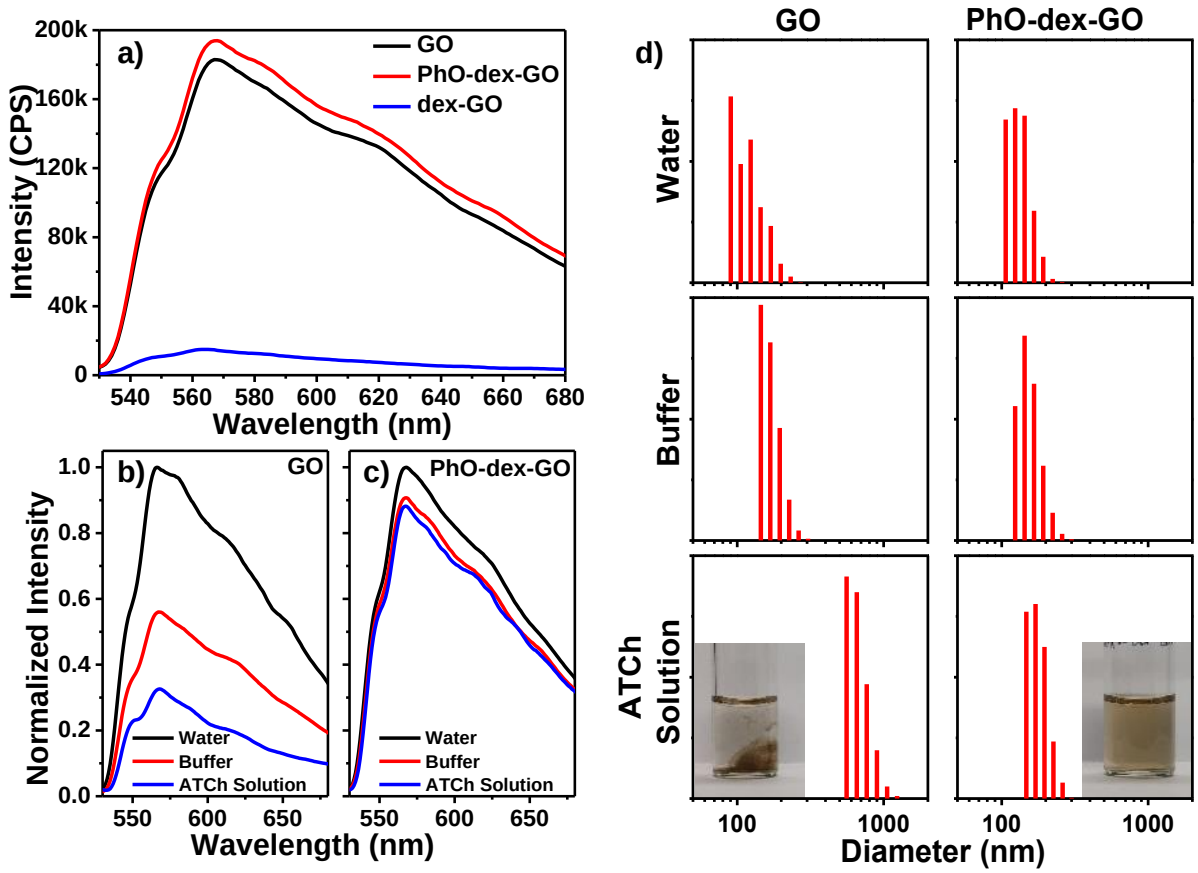

Figure 3. Fluorescence property of PhO-dex-GO and its colloidal stability. a) Fluorescence spectra of pristine GO, non-covalently functionalized PhO-dex-GO, and covalently-functionalized dex-GO at the same concentration (50 μg/mL). b) Fluorescence spectra of pristine GO and c) PhO-dex-GO in water, HEPES buffer, and an ATCh solution. d) Size distribution of GO and PhO-dex-GO as dispersed in water, HEPES buffer (5 mM), and an ATCh solution (19 mM), showing that non-covalently functionalized PhO-dex-GO maintained the same size distribution in all solutions while the size distribution of pristine GO shifted towards larger sizes in the HEPES buffer and ATCh solutions. The insets are photographs of GO and PhO-dex-GO dispersed in the ATCh solution.

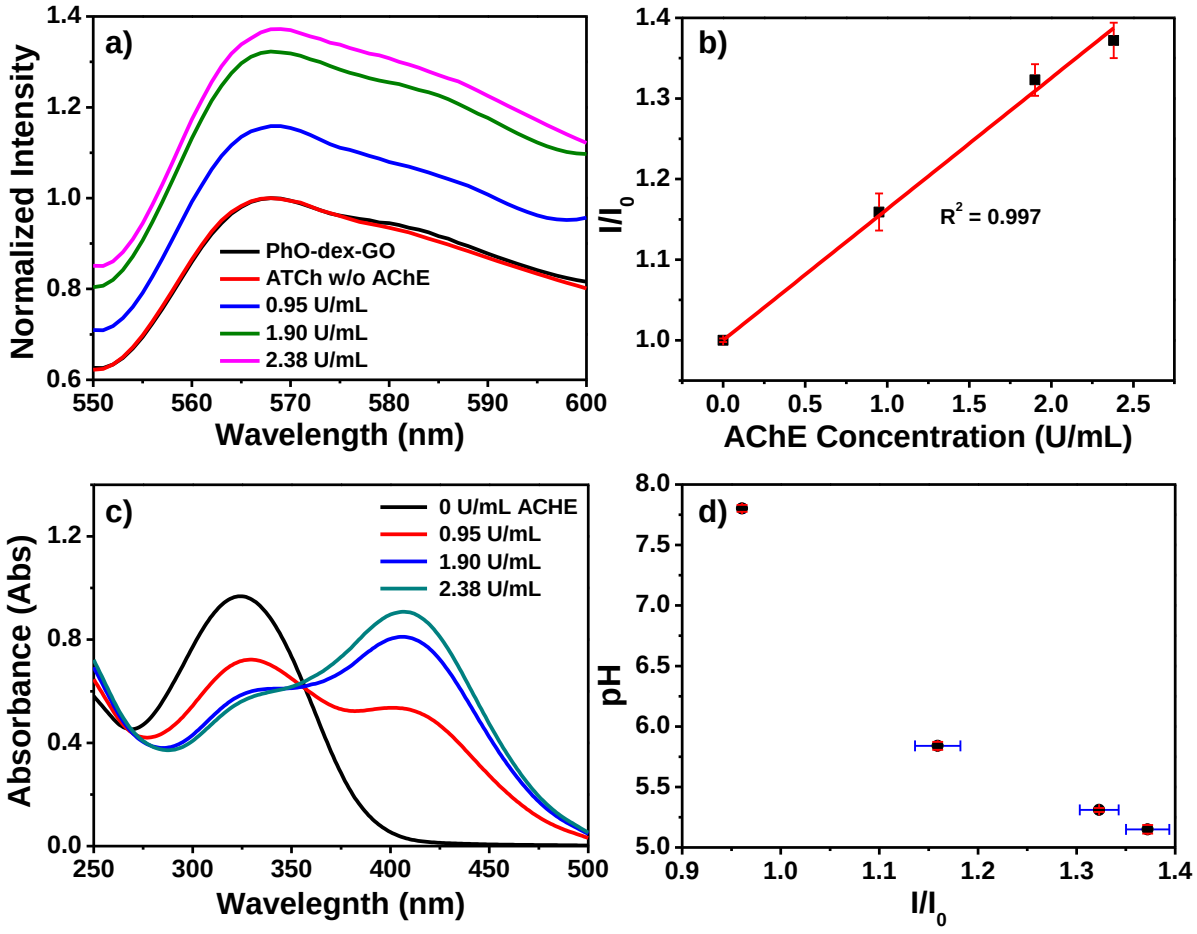

Figure 4. Fluorescence response of non-covalently functionalized PhO-dex-GO to the hydrolysis activity of AChE. a) Fluorescence spectra of PhO-dex-GO in the presence of AChE at various concentrations from 0.95 to 2.38 U/mL. A 19 mM of ATCh was added as a substrate. b) The change in fluorescence intensity of PhO-dex-GO at 568 nm as a function of AChE concentrations. I_0 and I are the fluorescence intensity of the PhO-dex-GO before and after the enzymatic hydrolysis of ATCh, respectively. c) UV-Vis absorption spectra of Ellman's reagent, 5,5'-dithiobis-(2-nitrobenzoic acid), to monitor the hydrolytic activity of AChE by measuring the absorbance at 412 nm. d) A plot of pH changes in the PhO-dex-GO solution against the fluorescence intensity changes of PhO-dex-GO during the enzymatic hydrolysis of ATCh at

various concentrations of AChE. All error bars represent standard deviation from the mean values (n = 4).

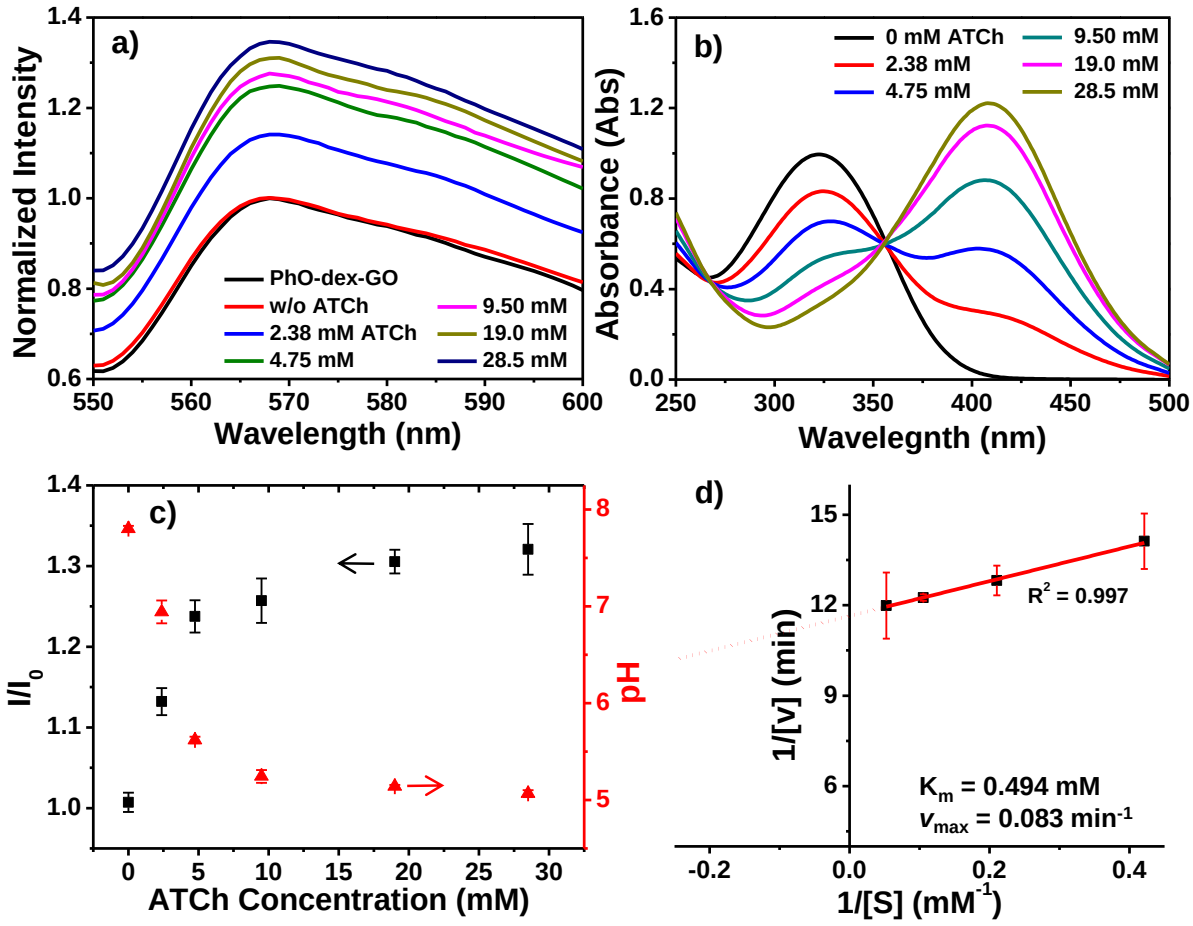

Figure 5. Fluorescence response of non-covalently functionalized PhO-dex-GO as a function of ATCh concentrations. a) Fluorescence spectra of PhO-dex-GO in the presence of ATCh at various concentrations from 2.38 to 28.5 mM. A 1.9 U/mL of AChE was used in the hydrolytic reactions of ATCh. b) UV-Vis absorption spectra of Ellman's reagent, 5,5'-dithiobis-(2-nitrobenzoic acid), to monitor the hydrolytic activity of AChE at various concentrations of ATCh by measuring the absorbance at 412 nm. c) Fluorescence intensity change of PhO-dex-GO at 568 nm (black square dots) and a pH change in the PhO-dex-GO solution (red triangle dots) following the enzymatic hydrolysis of ATCh at various concentrations. I_0 and I are the fluorescence intensity of the PhO-dex-GO before and after the enzymatic hydrolysis of ATCh, respectively. d) Lineweaver-Burk plot for the fluorescence response of PhO-dex-GO to the

hydrolytic activity of AChE (1.9 U/mL) at various concentrations of ATCh, providing the kinetic parameters for the enzymatic hydrolysis reaction of ATCh. All error bars represent standard deviation from the mean values (n = 4).

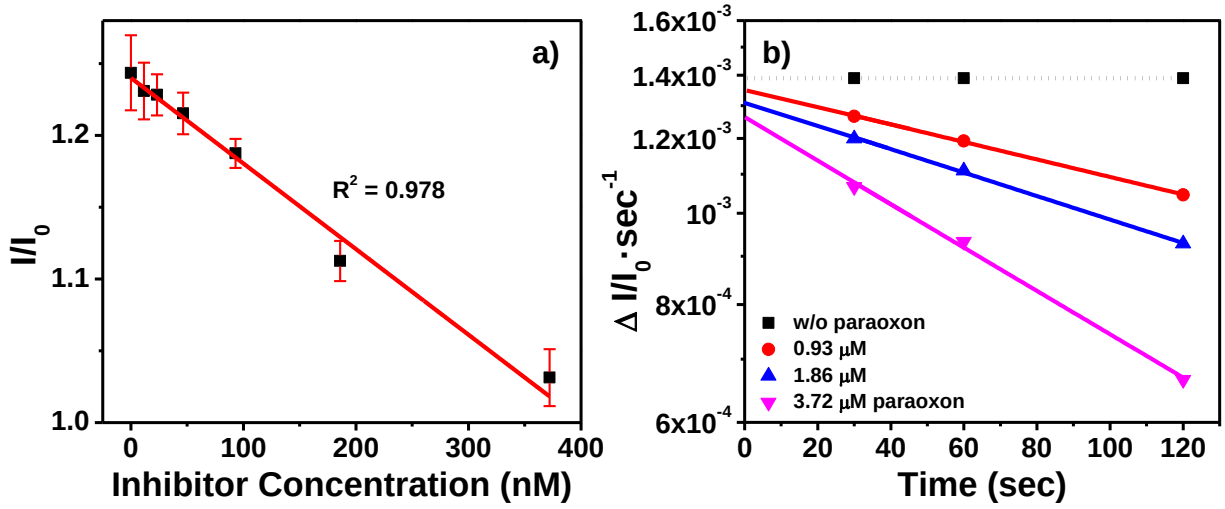

Figure 6. Optical detection of an AChE inhibitor on non-covalently functionalized PhO-dex-GO. a) Fluorescence response of PhO-dex-GO to the hydrolytic activity of AChE (1.9 U/mL) in the presence of its inhibitor, paraoxon, at various concentrations from 0 to 372 nM at 37 ºC. A 19 mM of ATCh was used in all enzymatic hydrolysis reactions. I_0 and I are the fluorescence intensity of PhO-dex-GO at 568 nm in the absence and presence of an inhibitor, respectively. All error bars represent standard deviation from the mean values (n = 4). b) Zero-Time plots of reaction velocities (Δ I/I_0 sec^{-1}) against time during inhibition of AChE (1.9 U/mL) at various concentrations of paraoxon in the presence of ATCh (19 mM) at 37 ºC. Regression lines were obtained by the least squares method.

TOC Figure

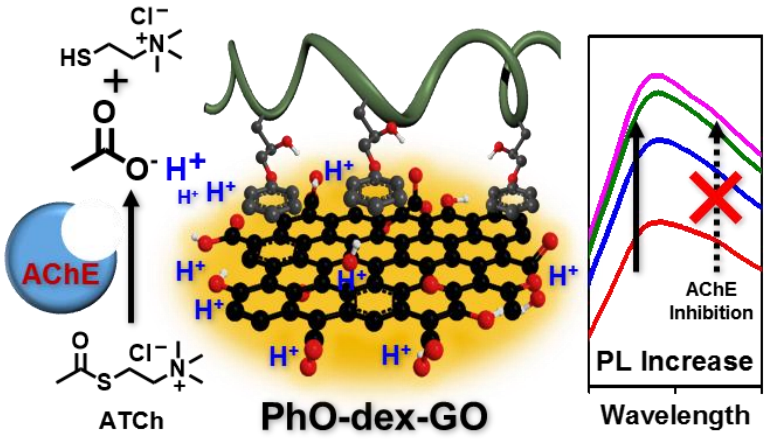
HS
Cl⁻
O
O⁻
H⁺
AChE
ATCh
PhO-dex-GO
AChE
Inhibition
PL Increase
Wavelength